Adsorption Kinetics of NIPAM-Based Polymers at the Air−Water Interface As Studied by Pendant Drop and Bubble Tensiometry

Vincent P. Gilcreest,*,†,‡ Kenneth A. Dawson,† and Alexander V. Gorelov†,§

Chemistry Department, University College Dublin, Belfield, Dublin 4, Ireland and Institute of Theoretical and Experimental Biophysics of the Russian Academy of Science, Puschino, Moscow region, 142 290, Russia

Received: June 30, 2006; In Final Form: August 24, 2006

The adsorption of *N*-isopropylacrylamide (NIPAM) based thermoresponsive polymers at the air−water interface was investigated by using drop and bubble shape tensiometry. The molecular weight dependence of polymer adsorption rate was studied by using narrowly distributed polymer fractions (polydispersity < 1.2) that were prepared by solvent:nonsolvent fractionation. The time-dependent surface tension profiles were fitted to the Hua−Rosen equation and the t^* values obtained were applied for interpretation of the kinetic data. It was found that the rate of polymer adsorption increased as the molecular weight of the polymer decreased. The relationship between polymer surface concentration and surface tension was determined by applying the pendant drop as a Langmuir-type film balance. From this relationship, the kinetics of polymer adsorption determined experimentally was compared with the adsorption rates predicted by a diffusion-controlled adsorption model based on the Ward−Tordai equation. The predicted adsorption rates were in good agreement with what was found experimentally. The dependence of the adsorption rate on the molecular weight of polymers can be satisfactorily described within the diffusion-controlled model.

Introduction

The properties of thermoresponsive polymers have received increasing interest in the literature, with a vast list of potential applications being cited. Poly(*N*-isopropylacrylamide) (PNIPAM) is perhaps the most popular member of this series. PNIPAM has a lower critical solution temperature (LCST) in water at ∼32 °C. An increase in the temperature of the solution to above the LCST changes PNIPAM from being hydrophilic to hydrophobic. PNIPAM has been applied in many different forms: single polymer chains, macroscopic gels, microgels, latexes, thin films, membranes, coatings, and fibers.[1] PNIPAM has also been grafted to a range of surfaces to create an intelligent surface that can be alternated from hydrophilic to hydrophobic by adjusting the temperature of the system.[2−6] These systems have been applied in a range of diverse areas, such as in chromatography,[7] microfluidic devices,[8,9] optical switching devices,[10,11] and as a substrate for cell culture.[4,12−16]

The interfacial properties of polymers have received a large amount of interest due to their role in the industrial and biological world. The ability of polymers to adsorb at an interface and modulate its properties has led to their use in a wide range of applications such as colloidal stability and coating processes, also the role of biopolymers such as proteins in biological processes such as cell adhesion and blood clotting has led to a host of potential uses in biotechnology. The absorption of PNIPAM at an interface is due to its amphiphilic structure that arises from its hydrophobic backbone and isopropyl group, and its hydrophilic amide group. The ability of PNIPAM to greatly reduce the surface tension at the air−water interface has led to increased interest in its use as a polymer surfactant. The magnitude of the decrease in the surface tension at the air−water interface is significantly greater (∼30 mJ/m^2)[17] than that of other aqueous polymers such as PEO (∼10 mJ/m^2)[18] and comparable to that of polymers commonly used as surfactants such as PPO−PEO−PPO copolymers (∼30−40 mJ/m^2).[19] PNIPAM is also interesting due to the possibility to control system parameters such as the rate of adsorption, the meso-equilibrium surface tension, and the total amount adsorbed at an interface by adjusting the temperature.

The surface properties of aqueous polymer solutions have been extensively investigated; however, until recently progress has been slow due to the lack of suitable experimental techniques. Recent advances in techniques such as surface laser light scattering[20] and neutron and X-ray scattering[21] have enabled a greater understanding of the structure of equilibrated adsorbed polymer films. However, these techniques are not suitable for characterization of the dynamic adsorption of polymers on an interface, as the time-scale for data collection is generally large relative to the time-scale for the adsorption process. The kinetics of polymer adsorption at an interface has been studied by using techniques such as surface plasmon resonance,[22,23] surface tension measurements,[24] and ellipsometry.[25,26] These techniques are not readily applicable to the air−water interface. Surface plasmon resonance is generally restricted to use at the solid−liquid interface and ellipsometry is not suitable for systems displaying high rates of adsorption as the time required for measurement is limiting.

The majority of the research into PNIPAM at the air−water interface has been carried out with polydisperse polymers. The use of polydisperse samples makes it difficult to interpret the results obtained about the rate of PNIPAM adsorption at an interface. In this work, narrowly dispersed PNIPAM fractions (PD < 1.2) were prepared by fractional precipitation. The dependence of the kinetics of adsorption on molecular weight

* Address correspondence to this author: vincent.gilcreest@NUIGalway.ie. Phone: 00353 (0) 87 6230977. Fax: 00353 (0) 91 494596.

† University College Dublin.

‡ Present address: NCBES, National University of Galway, Ireland.

§ Institute of Theoretical and Experimental Biophysics of the Russian Academy of Science.

10.1021/jp064112+ CCC: $33.50
Published on Web 10/11/2006

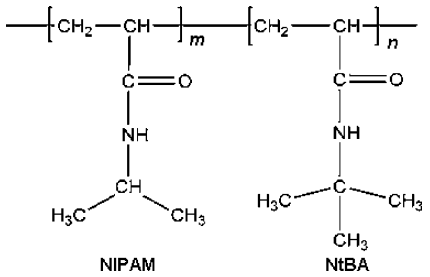

Figure 1. Chemical structure of PNIPAM and NIPAM/NtBA copolymer.

and concentration was obtained by using drop profile analysis tensiometry. Also the relationship between surface tension and the surface concentration of adsorbed polymer was obtained by applying the pendent drop method as a Langmuir-type film balance. The experimental kinetic data were compared with predicted data obtained by using a diffusion-controlled model. Finally, the adsorption rate of a copolymer with NtBA was compared with that of PNIPAM.

Materials and Methods

Materials. NIPAM (97%, Aldrich) and NtBA (purum, Fluka Chemie, Switzerland) were recrystallized from *n*-hexane and acetone, respectively. 2,2′-Azobis(2-methylpropionitrile) (AIBN) (Phase Separation LTD, Queensferry, Clwyd, UK) was recrystallized from methanol.

Acetone was shaken with anhydrous $CaSO_4$ (drierite) for 2 h. The decanted acetone was then distilled from fresh drierite. Ethanol was dried by reaction with magnesium ethoxide by addition of magnesium and iodine. The dried ethanol was then distilled off. Cyclohexane was distilled from sodium metal.

Polymer Synthesis and Fractionation. PNIPAM and poly(NIPAM(85)-*co*-NtBA(15)) (PN85) (where the number in parentheses is the molar percentage for the respective monomers) were prepared by free radical polymerization, using AIBN (0.5 mol % of AIBN per monomer) as an initiator in benzene under an argon atmosphere. Polymer structures are displayed in Figure 1. After polymerization at 60 °C for 24 h, the mixture was precipitated in cyclohexane. Precipitation was repeated three times with acetone as a solvent and cyclohexane as a nonsolvent, and the polymer was dried at room temperature under vacuum.

Narrowly dispersed polymer fractions were prepared by fractional precipitation. The polymer was dissolved in dry acetone (4 g/L). Dry cyclohexane was added dropwise until the solution became slightly turbid due to the formation of a precipitate. At this stage the addition was stopped. The solution was stirred for a further 20 min to allow equilibration. The solution was left for 24 h without stirring in a sealed flask to allow the precipitate to sediment to the bottom of the flask after which the clear supernatant was removed. The process of cyclohexane addition to the supernatant was repeated until the required number of fractions were obtained. Each fraction was dried under vacuum at 60 °C for 2 h.

Polymer Characterization. The molecular weight (M_w) and polydispersity (P.D.) of the polymers were determined by gel permeation chromatography (GPC), using a glucose bound polydivinylbenzene packed column (Jordi Assoc.) with DMF (0.25M LiBr) as the elution solvent. A series of monodisperse polystyrene polymers were used for calibration.

The *z*-average diffusion coefficient (D_z) was obtained for the polymer fractions with use of dynamic light scattering. Measurements were performed with a Malvern PCS-4700 instrument equipped with a Malvern correlator (7132). The 488.0 nm line of a Coherent Innova-70 Argon ion laser (Coherent, CA) was used for the incident beam. Round quartz cells with an outer diameter of 10 mm were used for measurements. The cells were immersed in a vat which contained water that was first distilled before passing through a Milli-Q filtration pack. The temperature of the water in the vat was maintained at a constant temperature (±0.02 °C) with an external RTE-221 microprocessor controlled circulating bath (Neslab, NH). The laser power used was between 100 and 300 mW. The scattering angles over which measurements were taken were in the range of 25−90°. Three measurements were taken at each angle and the results averaged. Data were analyzed by using the monomodal cumulants method. The D_z values reported were obtained by extrapolation to zero scattering angle and solution concentration.

The LCST's of the polymers were previously reported with use of differential scanning calorimetry.[12]

Surface Tension Measurements. Dynamic surface tension measurements were performed with a home-built goniometer based on the design and schematics described by Hansen.[27] The tensiometer was assembled on an optical rail from Newport Optics with optomechanical components from Newport Optics and Edmund Optics. Axisymmetric drop and bubble shape analysis was carried out with DROPimage software marketed by Rame Hart and developed by Hansen. The experimental drop or bubble profile was fitted to the theoretical profile generated by the numerical integration of the Young−Laplace equation, using surface tension as one of the adjustable parameters. The density of the polymer solutions was found to be equivalent to that of water within experimental error.

1. Adsorption. Kinetic experiments were carried out with a home-built pendant bubble tensiometer. The experimental system consisted of a stainless steel capillary with a U-shaped ending inserted into a polymer solution in a quartz cuvette that was mounted in a temperature-controlled cell with temperature control of ±0.1 °C. The steel capillary was attached to a valve so that the system could be isolated from external environmental influences. A short Teflon capillary with an outer diameter of 0.3175 cm and an inner diameter of 0.193 cm was inserted onto the end of the U-shaped tubing. In a typical experiment a bubble was formed on the tip of the Teflon capillary by using a plastic syringe. The system was then isolated by closing off the valve. Images were obtained every 1−3 s depending on experiment duration. Each measurement was repeated three times and the results were averaged.

2. Surface Expansion. For determination of the surface tension−surface concentration isotherm, a home-built pendant drop tensiometer was applied as a Langmuir trough. A drop was formed on the end of a Teflon capillary with an outside diameter of 0.3175 cm and an inside diameter of 0.193 cm. The drop was enclosed in a purpose built aluminum cell. The cell was comprised two sections, an inner section where the drop was formed and an outer section that was pressed against the windows with use of silicon as a sealant. The temperature was controlled with a separate water bath for each section. The outer section was kept at a temperature 0.5 °C higher than the inner section to prevent condensation. Both sections were maintained at a constant temperature (±0.1 °C). Images were obtained every 1−3 s depending on the length of the experiment. In a typical experiment, a drop was formed and was aged until the adsorbed polymer layer reached equilibrium as determined from the surface tension. The air−water interface was expanded until drop detachment.

Results

Characterization of Polymer Fractions. The characterization data for the polymer fractions are presented in Table 1.

TABLE 1: Characterization Data for Polymer Fractions Obtained at 20 °C

polymer	$10^6 M_w$[a]	PD (M_w/M_n)	R_h (nm)	$(10^{11}D)_z$ (m^2/s)	$10^6 M_w$[b]
PNIPAM					
PN1	3.3	1.13	75.4	0.28	4.9
PN2	2.7	1.24	45.9	0.47	2.0
PN3	0.93	1.16	23.9	0.90	0.61
PN4	0.53	1.25	17.6	1.2	0.35
PN5	0.30	1.14	13.5	1.6	0.22
PN85					
PN85Fr1	2.0	1.13	43.0	0.50	NA
PN85Fr2	1.2	1.14	29.7	0.72	NA
PN85Fr3	0.54	1.16	19.4	1.1	NA
PN85Fr4	0.20	1.14	13.7	1.6	NA

[a] Determined from GPC. [b] Molecular weight obtained from diffusion coefficient, using the scaling relationship determined by Zhou et al.[28]

The LCST's of PNIPAM and PN85 have previously been reported for unfractionated samples. PNIPAM and PN85 have LCST's of 32.9 and 25.1 °C, respectively.[12] The incorporation of NtBA into the polymer lowers the LCST of the polymer due to the increased hydrophobicity of the polymer. Polymer fractions in the M_w range of 3.3×10^6 to 3.0×10^5 were obtained for PNIPAM, and 2.0×10^6 to 1.9×10^5 for PN85 as determined from GPC. The fractions obtained were narrowly dispersed for both polymers with a polydispersity of ~1.2. The *z*-average diffusion coefficient was obtained for all the fractions from dynamic light scattering at 20 °C. The hydrodynamic radius of the fractions was calculated from the *z*-average diffusion coefficient by using the Stoke−Einstein relation. The molecular weight for the PNIPAM fractions was also determined from the *z*-average diffusion coefficient by using a relationship between the diffusion coefficient and the molecular weight obtained by Zhou et al. (D (m^2/s) $= k_D M^{-\alpha_D}$).[28] By a method of combining static and dynamic light scattering, Zhou et al. determined K_D and α_D to be 1.36×10^{-8} and 0.55 respectively at 20 °C. This relationship has been supported by experimental data from the Wu group[29,30] and Kubota et al.[31]

Concentration Dependence of Dynamic Surface Tension Profiles for PNIPAM. The adsorption of polymers at an interface has received extensive theoretical treatment with many models describing the adsorption process being proposed. The adsorption of a polymer on an interface consists of three main stages. The multistage adsorption process complicates the modeling of polymer adsorption on an interface. First the polymer must diffuse to the interface, second it must attach to the interface, and finally it has to spread itself. To gain some insight into the kinetics of PNIPAM adsorption at an interface, the dependence of the rate of surface tension lowering on solution concentration was carried out.

The Hua−Rosen equation (eq 1) has been extensively used in the literature for fitting to the time dependent surface tension and represents a convenient means for extracting information about the kinetics (t^*):

$$\log\frac{\gamma_s - \gamma(t)}{\gamma(t) - \gamma_m} = n \log\frac{t}{t^*} \quad (1)$$

where t^* is the time it takes for the surface pressure ($\gamma_0 - \gamma(t)$) to attain half its value at meso-equilibrium, $\gamma(t)$ is the surface tension at time t, γ_s is the surface tension the instant the drop is formed and is assumed equal to the surface tension of water (72.7 mJ/m^2 at 20 °C), n is an empirical constant, and γ_m is the meso-equilibrium surface tension. The experimental data were fitted to the Hua−Rosen equation by using the Marquardt−Levenberg algorithm implemented in SigmaPlot version 8.02. A good fit ($R^2 > 0.99$) was obtained for all the experimental data. In this work the reported γ_m was obtained as a fitting parameter to the Hua−Rosen equation and was determined to be 43.7 ± 0.5 mJ/m^2. This value is in agreement with previously reported equilibrium surface tensions of PNIPAM adsorbed layers at the air−water interface.[17,20,32−34] Typical Hua−Rosen fits are presented in Figure 2. Due to limitations in the experimental setup, t^* could not be obtained accurately below ~10 s. However, by use of the highest molecular weight sample PN1, t^* was accurately obtained for a wide concentration range (5−100 ppm).

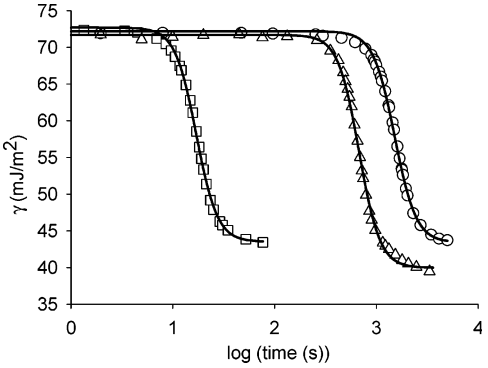

Figure 2. Hua−Rosen fits (—) to dynamic surface tension data for PN1 (10 ppm, ○), PN5 (50 ppm, □), and PN85Fr4 (25 ppm, △).

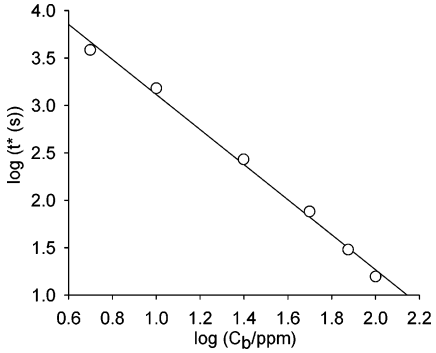

Figure 3. Concentration dependence of the half-time (t^*) for PN1-(○). The linear fit of the data is also shown in the graph (slope = −1.85).

It is clear that an increase in concentration leads to an increase in the rate of surface tension lowering, evidenced by t^* decreasing with solution concentration (Figure 3). For diffusion-controlled polymer adsorption, the Ward and Tordai equation can be used to determine the initial rate of adsorption.[35] The Ward and Tordai equation is presented below in modified form,[36] and the additional second term takes account of the different adsorption behavior present at a curved interface relative to a planar interface:

$$\Gamma(t) = 2(D/\pi)^{1/2}[C_0 t^{1/2} - \int_0^{\sqrt{t}} C_s(t-\tau)\, d\tau^{1/2}] + (D/b)[C_0 t - \int_0^t C_s(\tau)\, d\tau] \quad (2)$$

where C_0, C_s, and b are the bulk solution concentration, the concentration just below the interface, and the radius of the curvature, respectively. The negative terms allow for desorption from the interface and in the case of polymers this is insignificant. As the second term is generally negligible, at low surface concentration the Ward and Tordai equation can be applied in the following simplified form:

$$\Gamma = 2C_b\left(\frac{Dt}{\pi}\right)^{1/2} \quad (3)$$

The Ward and Tordai equation predicts that the time for a certain surface coverage to be reached is proportional to $(1/C_b)^2$. Figure 3 shows $\log(t^*)$ versus $\log(C_b)$ for PNIPAM. For diffusion-controlled polymer adsorption the Ward and Tordai equation predicts a slope of -2. The slope obtained for PN1 (-1.85) was in good agreement with the predicted value.

Development of the Diffusion-Controlled Model. From our investigation into the concentration dependence of the half-time for PN1, it is evident that the adsorption rate for PN1 is diffusion controlled over the concentration range investigated. However, it cannot be concluded from this investigation that the rate of adsorption for PNIPAM will always be diffusion controlled. For example, at sufficiently high concentrations, diffusion to the interface will be almost an instantaneous event, and in these conditions the rate will be controlled by some other adsorption stage, such as attachment to the interface or spreading. Also, the rate-determining stage could be dependent on polymer molecular weight. In the following section, the rate of PNIPAM adsorption will be compared with adsorption rates predicted by a diffusion-controlled model. The model applied is based on the Ward−Tordai equation and predicts the surface concentration versus time. As the experimental data that was obtained is the change of surface tension with time, a relationship between the surface tension and surface concentration must be obtained.

A number of groups have previously determined this relationship by using various techniques. Kawaguchi et al. determined the relationship between the surface pressure of a PNIPAM film and the surface concentration at 16 and 31.6 °C using a Langmuir trough.[37,38] Pelton et al. fitted the Kawaguchi data to an analytical equation to determine the functional relationship between the surface tension and the surface concentration.[24] A different approach was adopted here for determining the relationship between the surface tension and the surface concentration of PNIPAM at the interface. Briefly, a pendant drop in which the interface had reached its meso-equilibrium surface tension was expanded (a pendent drop was used in preference to a bubble for creating the isotherm due to the greater stability in the surface area achievable). From the drop expansion experiment the relationship between the surface tension and the relative surface area (A/A_{ref}) was obtained. From this relationship it was possible to determine the relationship between the surface tension and relative surface concentration (Γ_{ref}/Γ), from which a functional relationship between surface tension and surface concentration was obtained by fitting to the kinetic data. The process is described in greater detail below.

An isotherm of surface tension against ($A_{ref}/A(t)$) (where $A(t)$ is the surface area at time t and A_{ref} is a reference surface area defined by the area at which drop expansion is started) can be determined by expanding a drop with polymer adsorbed at the interface. Drop expansion was carried out at a range of expansion rates, from 0.1 to 3 mm^2/s, and similar isotherms were obtained with any differences observed been within experimental error. This is a consequence of the use of a high molecular weight sample at low solution concentration, therefore minimizing polymer adsorption during the experiment. For the purpose of this work an expansion rate of 0.3 mm^2/s was selected and it was estimated that less than 0.1 mg/m^2 of polymer adsorbs during expansion, based on an expansion time of 150 s and applying the Ward−Tordai equation (eq 2). It was desirable that the drop interface reached its meso-equilibrium surface tension before expansion was begun so that an extended curve could be obtained. Drop expansion was started 2 h after drop formation at which stage the surface tension was ~43 mJ/m^2 (Figure 4a). Figure 4a can be rescaled in terms of $\Gamma/\Gamma_{ref(2h)}$ (Figure 4b) by using

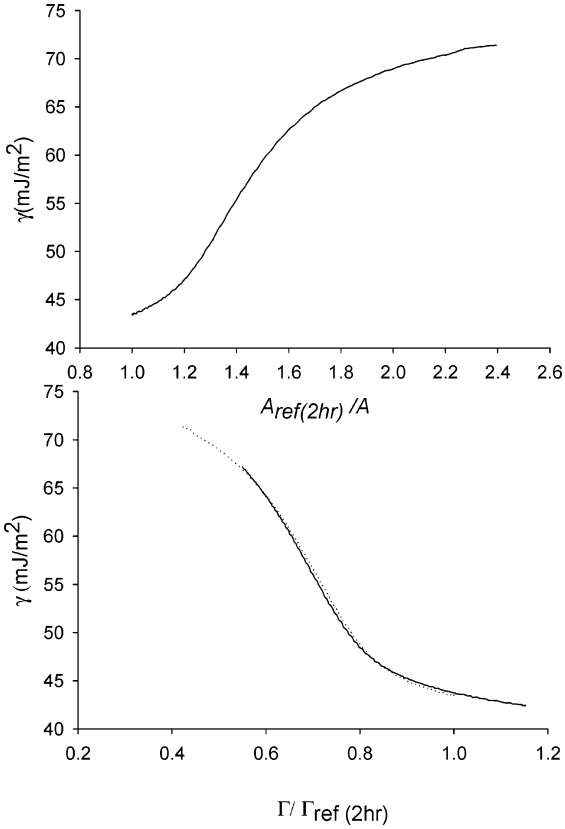

Figure 4. (a) Surface tension versus A_{ref}/A isotherm obtained when drop expansion was started after 2 h. (b) Comparison of isotherms obtained after 2 h (···) and 3 h (—) adsorption time.

$$\frac{A_{ref}}{A} = \frac{\Gamma}{\Gamma_{ref(2h)}} \quad (4)$$

where $\Gamma_{ref(2h)}$ is the surface concentration when drop expansion is started after 2 h. To investigate the effect of Γ_{ref} on isotherm shape, the experiment was repeated with the drop expansion started after 3 h (Figure 4b). For comparison purposes, the isotherm obtained after 3 h was rescaled in terms of $\Gamma/\Gamma_{ref(2h)}$ by using

$$\frac{\Gamma}{\Gamma_{ref(2h)}} = \frac{\Gamma}{\Gamma_{ref(3h)}}\frac{\Gamma_{ref(3h)}}{\Gamma_{ref(2h)}} \quad (5)$$

where the ratio $\Gamma_{ref(3h)}/\Gamma_{ref(2h)}$ was determined to be 1.153 (method described later). From Figure 4b it can be seen that the shape of the isotherm is independent of Γ_{ref}. The isotherm obtained after 2 h was selected for further analysis.

The isotherm obtained from PN1 was applied to the full molecular weight range, which was possible due to the weak molecular weight dependence of the isotherm. The weak dependence of the $\pi-\Gamma$ isotherm on molecular weight has been found experimentally.[18,39−41] This weak dependence is perhaps not surprising. At low surface concentration, the $\pi-\Gamma$ isotherm is dependent on the molecular weight;[42] however, in the dilute regime there is very little change in the surface pressure and any contribution due to different molecular weights will be within experimental error (<0.1 mJ/m^2).[39] Above the concentration where the polymer chains begin to overlap (c^*), the

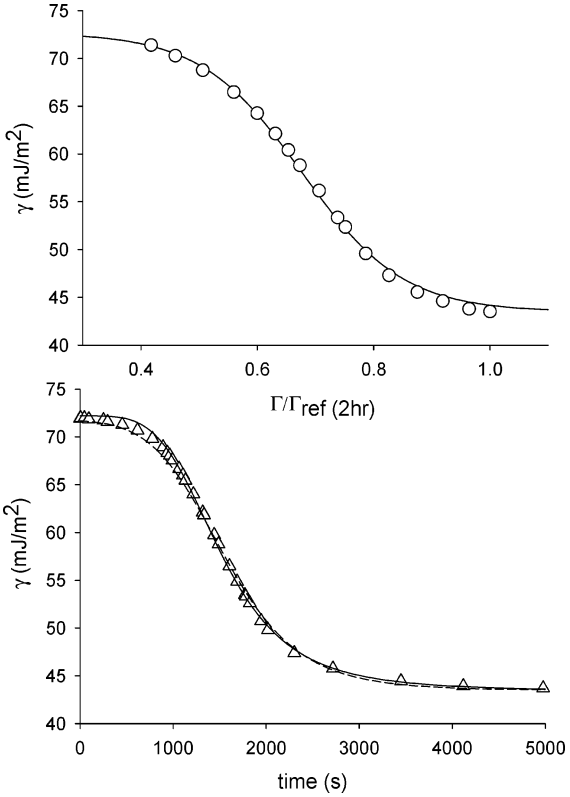

Figure 5. (a) Fit of eq 9 to the $\gamma-\Gamma/\Gamma_{ref}$ isotherm (○). (b) Fit of eq 10 (---) to experimental DST (△) for PN1 (solution concentration 10 ppm). Also shown is the fit of DST to the Hua−Rosen equation (—).

isotherm is independent of molecular weight and the relationship between the surface pressure and concentration is expressed by

$$\pi \approx \Gamma^{y} \tag{6}$$

with

$$y = 2\nu/(2\nu - 1) \tag{7}$$

where υ is the Flory exponent used to express the radius of gyration in terms of molecular weight ($R_g \approx M^{\nu}$) and is a measure of the quality of the solvent.[43]

For application of the $\pi-\Gamma$ isotherm in the kinetic modeling of PNIPAM adsorption, the isotherm is required in a functional form. Different functional dependencies were tested but the function proposed by Zhang and Pelton provided the best fit to the isotherm (eq 8).[24]

$$\gamma(\Gamma) = \mathrm{A} + \frac{B}{1 + C\mathrm{e}^{N\Gamma}} \tag{8}$$

As C is generally a small number, A ($\sim\gamma_m$) and B ($\sim\gamma_0 - \gamma_m$) were determined working in the limiting case of zero adsorption and complete adsorption. The constants C and N were obtained through fitting to the experimental data. However, the isotherm that was obtained experimentally was $\gamma-\Gamma/\Gamma_{ref}$, and not $\gamma-\Gamma$. The equation that was used for fitting is expressed below:

$$\gamma(\Gamma/\Gamma_{ref}) = \mathrm{A} + \frac{B}{1 + C\mathrm{e}^{N^*\Gamma}} \tag{9}$$

where $N^* = N\Gamma_{ref}$. With $A = 43.49$ mJ/m^2 and $B = 29.21$ mJ/m^2 (determined experimentally), eq 9 was fitted to the experimentally determined $\gamma-\Gamma/\Gamma_{ref}$ isotherm (Figure 5a). C and N^* were determined to be $4.1259e^{-4}$ and 11.5 ± 0.06, respectively.

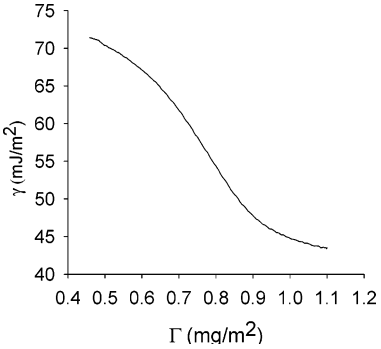

Figure 6. Experimental $\Gamma-\gamma$ isotherm obtained by using the determined Γ_{ref} value.

For diffusion-controlled surface tension lowering an expression for the dynamic surface tension can be obtained by combining the modified Ward and Tordai equation with eq 9:

$$\gamma(t) = A + \frac{B}{1 + C\mathrm{e}^{(N/\Gamma_{ref})(2C_b(Dt/\pi)^{1/2}+(D/b)C_bt)}} \tag{10}$$

The value of Γ_{ref} can now be determined by fitting to the experimental dynamic surface tension data. The dynamic surface tension data from PN1 with a solution concentration of 10 ppm were used for fitting. Due to the high molecular weight of PN1 and the low solution concentration used, it was assumed that the rate of surface tension lowering was diffusion controlled. The dynamic surface tension profile obtained from a 10 ppm solution of PN1 was fitted to eq 10 (Figure 5b).

From the fit, Γ_{ref} was determined to be 1.10 mg/m^2. It is important to note that even though drop expansion was started after the meso-equilibrium surface tension was reached, Γ_{ref} is not the surface concentration for an equilibrated PNIPAM layer. This can be seen clearly as the Γ_{ref} obtained when drop expansion was started after 3 h was 1.27 mg/m^2. It is evident that PNIPAM still absorbs on the interface after the meso-equilibrium surface tension is reached. This is commonly encountered in surface tension analysis of polymers at an interface. From the literature,[33,34,44] the equilibrium surface concentration for PNIPAM is in the range 1.5−2 mg/m^2.

By using the value for Γ_{ref} obtained, the $\gamma-\Gamma$ isotherm is presented in Figure 6. For comparison purposes and method validation, the surface concentration at the half-point ($(\gamma_0 - \gamma_m)/2$) was compared with existing data in the literature as it is in this region that the surface tension is most sensitive to surface concentration. Also the half-point will be the reference point that will be used for kinetic studies. From the $\Gamma-\gamma$ isotherm obtained in this work the half-point was determined to be 0.75 mg/m^2 (Γ^*). This value is comparable to the half-point that was obtained from Kawaguchi data where they determined the $\Gamma-\gamma$ isotherm using a Langmuir trough. In contrast to the method adopted in this work, the isotherm was obtained from equilibrated polymer films. The surface concentration at the half-point was estimated from their data[37] to be ~0.60 mg/m^2. A dynamic isotherm was obtained in this work and this may explain the discrepancy.

From the $\Gamma-\gamma$ isotherm it is possible to determine the Flory exponent υ for PNIPAM at the interface by using eqs 6 and 7. From a log−log plot of surface pressure (π) against surface concentration ($\log(\pi) = y \log(\Gamma)$) the slope is equal to y. A value of 4.57 was obtained for y, and from eq 7 the value of υ was determined to be 0.64 (Figure 7). This value is intermediate

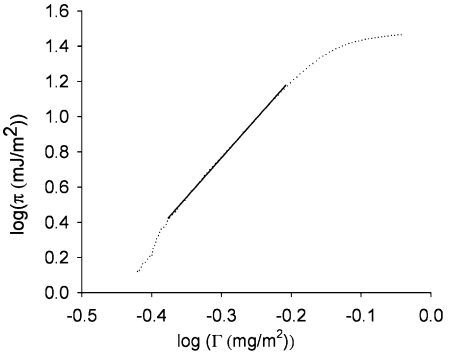

Figure 7. Double logarithmic plot of surface pressure versus surface concentration. Linear fit was carried out to the central portion of the curve that is described by eq 6.

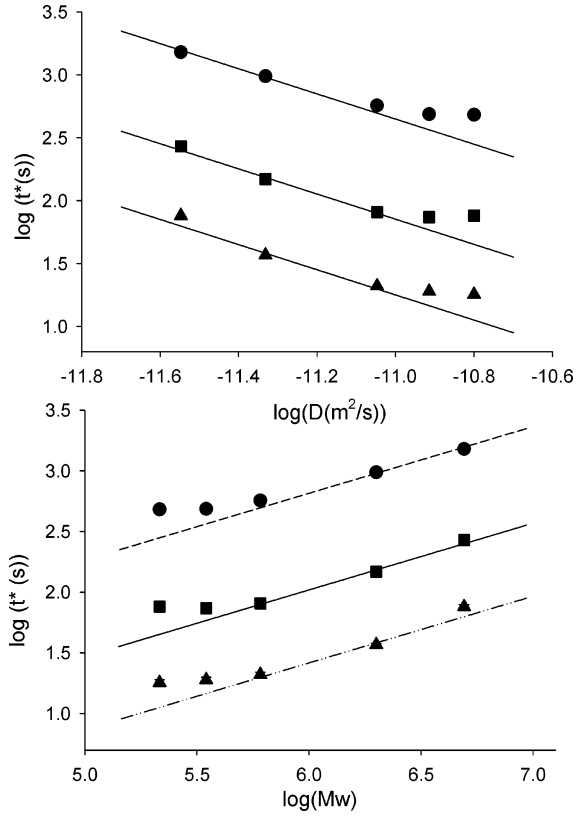

Figure 8. Comparison of experimental log(t^*) with predicted log(t^*) from diffusion model a sa function of (a) log(D) and (b) log(M_w) at 10 (●), 25 (■), and 50 ppm (▲). Solid lines are predicted values obtained from eq 10.

between the value of υ predicted for a good solvent (0.77) and a θ solvent (0.505).[45]

Comparison of Dynamic Surface Tension Predicted by Using a Diffusion-Controlled Model with Experimental Data. By obtaining the diffusion coefficients for each fraction from light scattering data (Table 1) and applying eq 10, the diffusion-controlled dynamic surface tension profiles were predicted. For comparison of the rate of surface tension lowering obtained experimentally and the rate of surface tension lowering predicted by using the diffusion-controlled model (eq 10), the predicted t^* was determined to be 57.9 mJ/m^2 based on previously defined values for A and B. The predicted half-times were compared with the experimentally obtained t^* as a function of diffusion coefficient (Figure 8a) and molecular weight (Figure 8b) by using the Zhou coefficients.[28] There is good agreement between predicted and experimentally determined rates indicating that

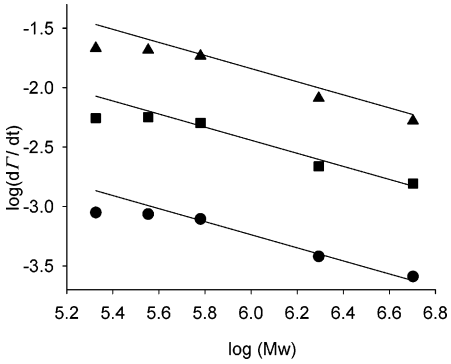

Figure 9. Comparison of experimental log(dΓ/dt) with predicted log(dΓ/dt) as a function of log(Mw) at 10 ppm (●), 25 ppm (■) and 50 ppm (p). Solid lines are predicted values obtained from eq 14 with Γ^* =0.75 mg/m^2.

the rate of surface tension lowering for PNIPAM at the air−water interface is diffusion controlled.

The rate of polymer adsorption was also compared with predicted rates. Adsorption rates were obtained from the dynamic surface tension and the $\gamma-\Gamma$ isotherm (Figure 6) by using the following relationship:

$$\frac{d\Gamma}{dt} = \frac{d\Gamma}{d\gamma}\frac{d\gamma}{dt} \tag{11}$$

For diffusion-controlled adsorption, the rate can be obtained from the simplified Ward and Tordai equation (eq 3):

$$\frac{d\Gamma}{dt} = c\sqrt{\frac{D}{\pi t}} \tag{12}$$

From eq 3, t can be rewritten in terms of Γ and D:

$$t = 4\left(\frac{\Gamma}{c}\right)^2\frac{\pi}{D} \tag{13}$$

The adsorption rate at a certain surface concentration was obtained by combining eqs 12 and 13:

$$\frac{d\Gamma}{dt} = \frac{2Dc^2}{\pi\Gamma} \tag{14}$$

The experimental and predicted adsorption rates were obtained at Γ^* by using eqs 11 and 14 (Figure 9). Once again there is good agreement between experimental and predicted data.

Kinetics of Adsorption for a NIPAM:NtBA Copolymer. The kinetics of adsorption for a NIPAM:NtBA copolymer was also investigated. The concentration analysis presented for PN1 (Figure 3) was also carried out for PN85Fr1. The slope obtained was significantly lower (−1.31) than was predicted by eq 3 (slope −2). It is also noticeable from Figure 10 that PN85 displays an apparent reduced rate of surface tension lowering than PNIPAM. This is attributed to PN85 having a higher surface concentration as witnessed from preliminary findings and is currently the source of extended research within the group. Incorporation of NtBA also led to a reduction in the meso-equilibrium surface tension ($\gamma_m = 40.1 \pm 0.5$mJ/m^2) due to the increased hydrophobicity of the copolymer.

Discussion

The experimentally observed kinetics of PNIPAM adsorption were in good agreement with the diffusion-controlled model; however, it is noticeable that at lower molecular weight, the rate of polymer adsorption was lower than was predicted by

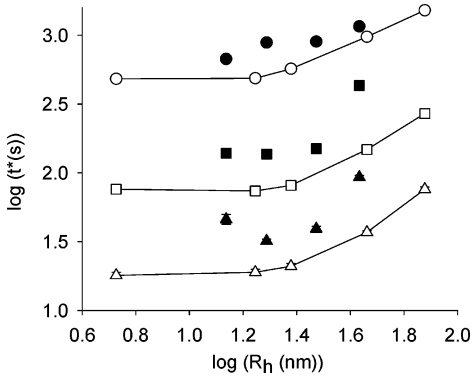

Figure 10. Dependence of the half-time (t^*) for PNIPAM (line and open symbols) and PN85 (solid symbols) on hydrodynamic radius at 10 (●, ○), 25 ppm (■, □) and 50 ppm (▲, △).

the model. It is apparent that in this regime, the kinetics of polymer adsorption are only weakly dependent on molecular weight. This finding can be explained by the mechanism of adsorption. The adsorption of a polymer at an interface involves two main stages, diffusion to the interface followed by attachment and rearrangement on the interface. The rate of diffusion is clearly dependent on molecular weight. However, the dependence of polymer attachment and rearrangement on molecular weight is more complicated. A number of experimental and theoretical investigations have been carried out into the molecular weight dependence of polymer adsorption. De Gennes predicted that the polymer spreading time, τ_s, scales with N^2 (N is the degree of polymerization) based on a reptation model.[46] Semenov and Joanny investigated polymer adsorption rates using Rouse−Zimm dynamics for the polymer chains.[47] The calculations were carried out in two regimes: (1) adsorption to a preadsorbed interface close to saturation and (2) adsorption to a strongly starved interface. In the case of adsorption to a preadsorbed interface, similar molecular weight dependencies to de Gennes were proposed; however, they report the adsorption rate to be independent of molecular weight in the case of a strongly starved interface. Similar findings were also reported by Ligoure and Leibler.[48]

In principle, our experimental results do not contradict the above theoretical finding, if we assume that the amount of adsorbed polymer is well below saturation (starved interface). In that case, one does not observe any molecular weight dependence after the diffusion was taken into account. The shape of the $\gamma-\Gamma$ isotherm shows that most changes in the surface tension occur in a relatively narrow range of Γ. From the drop expansion experiments we can conclude that above $\Gamma \sim 1$ mg/m^2 the polymer continues to adsorb in large amounts with little change in surface tension. That is, the surface tension reflects the changes in the amount of adsorbed polymer only well below the saturation of the interface. The dependence of adsorption rate on molecular weight could still exist for $\Gamma > 1$ mg/m^2. However, this range of surface densities cannot be observed with surface tension measurements.

The investigation of the dynamics of polymer adsorption at an interface has been limited due to a lack of suitable experimental techniques. Common techniques employed for studying adsorbed polymer layers such as surface plasmon resonance are not suitable for characterization of the dynamic adsorption of polymers at the air−water interface. Also techniques such as ellipsometry are limited as the time-scale for data collection is generally large relative to the time-scale for the adsorption process. Due to difficulties in applying existing experimental techniques to the air−water interface, polymer adsorption rates have mainly been reported at the solid−liquid interface. Fu et al. investigated the molecular weight dependence of the kinetics of polystyrene adsorption from dilute θ solutions onto gold using a quartz crystal balance.[49] Contrary to existing adsorption theories, the adsorption rate was independent of molecular weight. No explanation for this behavior was presented. A similar finding was also reported by Xie and Granick, who investigated the adsorption of poly(methacrylic acid) onto phospholipid bilayers of 1,2-dimyristoyl-*sn*-glycero-3-phosphocholine (DMPC) using FTIR.[50] The above references described the rate of adsorption on a solid surface at surface densities which are much higher than we could observe with surface tension. We point out that there is some experimental evidence in the literature that the adsorption rate can be independent of the molecular weight of polymer even at high surface densities.

Conclusions

In this work, pendant drop tensiometry was used to investigate the adsorption kinetics of thermoresponsive polymers at the air−water interface. The use of narrowly dispersed fractions enabled a comprehensive study into the mechanism of polymer adsorption at the interface to be carried out. The dynamic surface tension was obtained for narrowly dispersed fractions over a range of concentrations and it is evident that the adsorption rate is dependent on polymer molecular weight and solution concentration. Highest adsorption rates were observed for low molecular weight fractions and at higher solution concentrations, as expected. The relationship between surface tension (γ) and surface concentration (Γ) was obtained for PNIPAM by applying the pendant-drop technique as a Langmuir-type film balance. The isotherm was comparable with previous isotherms reported that were obtained by using a standard Langmuir trough. Using the functional relationship obtained from the $\gamma-\Gamma$ isotherm, a diffusion-controlled model based on the Ward and Tordai equation was used to predict the dynamic surface tensions for the PNIPAM samples over a range of molecular weights and concentrations. The predicted adsorption rates were in good agreement with the experimental data indicating PNIPAM adsorbs at the air−water in a diffusion-controlled manner. The incorporation of NtBA in the polymer structure decreases the adsorption rate comparable to PNIPAM homopolymer with the same diffusion coefficient.

References and Notes

(1) Schild, H. G. *Prog. Polym. Sci.* **1992**, *17*, 163.
(2) Wang, Y.-P.; Yuan, K.; Li, Q.-L.; Wang, L.-P.; Gu, S.-J.; Pei, X.-W. *Mater. Lett.* **2005**, *59*, 1736.
(3) Liu, J.; Pelton, R.; Hrymak, A. N. *J. Colloid Interface Sci.* **2000**, *227*, 408.
(4) Cunliffe, D.; Alarcon, C. D.; Peters, V.; Smith, J. R.; Alexander, C. *Langmuir* **2003**, *19*, 2888.
(5) Takei, Y. G.; Aoki, T.; Sanui, K.; Ogata, N.; Sakurai, Y.; Okano, T. *Macromolecules* **1994**, *27*, 6163.
(6) Yakushiji, T.; Sakai, K.; Kikuchi, A.; Aoyagi, T.; Sakurai, Y.; Okano, T. *Langmuir* **1998**, *14*, 4657.
(7) Kanazawa, H.; Kashiwase, Y.; Yamamoto, K.; Matsushima, Y.; Kikuchi, A.; Sakurai, Y.; Okano, T. *Anal. Chem.* **1997**, *69*, 823.
(8) Burns, M. A.; Mastrangelo, C. H.; Sammarco, T. S.; Man, F. P.; Webster, J. R.; Johnson, B. N.; Foerster, B.; Jones, D.; Fields, Y.; Kaiser, A. R.; Burke, D. T. *Proc. Natl. Acad. Sci. U.S.A.* **1996**, *93*, 5556.
(9) Huber, D. L.; Manginell, R. P.; Samara, M. A.; Kim, B. I.; Bunker, B. C. *Science* **2003**, *301*, 352.
(10) Reese, C. E.; Mikhonin, A. V.; Kamenjicki, M.; Tikhonov, A.; Asher, S. A. *J. Am. Chem. Soc.* **2004**, *126*, 1493.
(11) Jones, C. D.; Lyon, L. A. *J. Am. Chem. Soc.* **2003**, *125*, 460.
(12) Rochev, Y.; Golubeva, T.; Gorelov, A.; Allen, L.; Gallagher, W. M.; Selezneva, I.; Gavrilyuk, B.; Dawson, K. A. *J. Mater. Sci.: Mater. Med.* **2001**, *15*, 513.

(13) Rochev, Y.; O'Halloran, D.; Gorelova, T.; Gilcreest, V.; Selezneva, I.; Gavrilyuk, B.; Gorelov, A. *J. Mater. Sci.*: *Mater. Med.* **2004**, *15*, 513.
(14) Allen, L. T.; Fox, E. J. P.; Blute, I.; Kelly, Z. D.; Rochev, Y.; Keenan, A. K.; Dawson, K. A.; Gallagher, W. M. *Proc. Natl. Acad. Sci. U.S.A.* **2003**, *100*, 6331.
(15) Akiyama, Y.; Kikuchi, A.; Yamato, M.; Okano, T. *Langmuir* **2004**, *20*, 5506.
(16) Ito, Y.; Chen, G. P.; Guan, Y. Q.; Imanishi, Y. *Langmuir* **1997**, *13*, 2756.
(17) Zhang, J.; Pelton, R. *Colloids Surf., A* **1999**, *156*, 111.
(18) Sauer, B. B.; Yu, H. *Macromolecules* **1989**, *22*, 786.
(19) Munoz, M. G.; Monroy, F.; Ortega, F.; Rubio, R. G.; Langevin, D. *Langmuir* **2000**, *16*, 1083.
(20) Huang, Q. R.; Wang, C. H. *Langmuir* **1999**, *15*, 634.
(21) Russell, T. P. *Phys. B* **1996**, *221*, 267.
(22) Huang, Y. W.; Gupta, V. K. *Langmuir* **2002**, *18*, 2280.
(23) Brandani, P.; Stroeve, P. *Macromolecules* **2003**, *36*, 9502.
(24) Zhang, J.; Pelton, R. *Langmuir* **1999**, *15*, 5662.
(25) Awan, M. A.; Dimonie, V. L.; OuYang, D.; ElAasser, M. S. *Langmuir* **1997**, *13*, 140.
(26) Motschmann, H.; Stamm, M.; Toprakcioglu, C. *Macromolecules* **1991**, *24*, 3681.
(27) Myrvold, R.; Hansen, F. K. *J. Colloid Interface Sci.* **1998**, *207*, 97.
(28) Zhou, S. Q.; Fan, S. Y.; Auyeung, S. C. F.; Wu, C. *Polymer* **1995**, *36*, 1341.
(29) Zhang, G. Z.; Wu, C. *J. Am. Chem. Soc.* **2001**, 123, 1376.
(30) Wang, X. H.; Qiu, X. P.; Wu, C. *Macromolecules* **1998**, *31*, 2972.
(31) Kubota, K.; Fujishige, S.; Ando, I. *J. Phys. Chem.* **1990**, *94*, 5154.
(32) Jean, B.; Lee, L. T.; Cabane, B. *Langmuir* **1999**, *15*, 7585.
(33) Lee, L. T.; Jean, B.; Menelle, A. *Langmuir* **1999**, *15*, 3267.
(34) Kawaguchi, M.; Hirose, Y.; Kato, T. *Langmuir* **1996**, *12*, 3523.
(35) Ward, A.; Tordai, L. *J. Chem. Phys.* **1961**, *63*, 473.
(36) Lee, Y. C.; Lin, S. Y.; Liu, H. S. *Langmuir* **2001**, *17*, 6196.
(37) Kawaguchi, M.; Saito, W.; Kato, T. *Macromolecules* **1994**, *27*, 5882.
(38) Saito, W.; Mori, O.; Ikeo, Y.; Kawaguchi, M.; Imae, T.; Kato, T. *Macromolecules* **1995**, *28*, 7945.
(39) Poupinet, D.; Vilanove, R.; Rondelez, F. *Macromolecules* **1989**, *22*, 2491.
(40) Brinkhuis, R. H. G.; Schouten, A. J. *Macromolecules* **1991**, *24*, 1487.
(41) Kawaguchi, M.; Komatsu, S.; Matsuzumi, M.; Takahashi, A. *J. Colloid Interface Sci.* **1984**, *102*, 356.
(42) Llopis, J.; Subirana, J. A. *J. Colloid Sci.* **1961**, *16*, 618.
(43) Vilanove, R.; Rondelez, F. *Phys. Rev. Lett.* **1980**, *45*, 1502.
(44) Richardson, R. M.; Pelton, R.; Cosgrove, T.; Zhang, J. *Macromolecules* **2000**, *33*, 6269.
(45) Takahashi, A.; Yoshida, A.; Kawaguchi, M. *Macromolecules* **1982**, *15*, 1196.
(46) De Gennes, P. G. *C. R. Acad. Sci.* **1985**, *301*, 1399.
(47) Semenov, A. N.; Joanny, J. F. *J. Phys. II* **1995**, *5*, 859.
(48) Ligoure, C.; Leibler, L. *J. Phys.* **1990**, *51*, 1313.
(49) Fu, T. Z.; Stimming, U.; Durning, C. J. *Macromolecules* **1993**, *26*, 3271.
(50) Xie, A. F.; Granick, S. *Nature Mater.* **2002**, *1*, 129.